Biochemical Characterization of a Phosphinate Inhibitor of *Escherichia coli* MurC

Stephen Marmor,[‡] Christian P. Petersen,[‡,§] Folkert Reck,[||] Wei Yang,[⊥] Ning Gao,[‡] and Stewart L. Fisher*[,‡]

Departments of Biochemistry and Protein Science, Chemistry, and Molecular Sciences, Infection Discovery, Cancer and Infection Research Area, AstraZeneca R&D Boston, Waltham, Massachusetts 02451

Received July 5, 2001; Revised Manuscript Received August 10, 2001

ABSTRACT: The bacterial UDP-*N*-acetylmuramyl-L-alanine ligase (MurC) from *Escherichia coli*, an essential, cytoplasmic peptidoglycan biosynthetic enzyme, catalyzes the ATP-dependent ligation of L-alanine (Ala) and UDP-*N*-acetylmuramic acid (UNAM) to form UDP-*N*-acetylmuramyl-L-alanine (UNAM-Ala). The phosphinate inhibitor **1** was designed and prepared as a multisubstrate/transition state analogue. The compound exhibits mixed-type inhibition with respect to all three enzyme substrates (ATP, UNAM, Ala), suggesting that this compound forms dead-end complexes with multiple enzyme states. Results from isothermal titration calorimetry (ITC) studies supported these findings as exothermic binding was observed under conditions with free enzyme (K_d = 1.80−2.79 μM, 95% CI), enzyme saturated with ATP (K_d = 0.097−0.108 μM, 95% CI), and enzyme saturated with the reaction product ADP (K_d = 0.371−0.751 μM, 95% CI). Titrations run under conditions of saturating UNAM or the product UNAM-Ala did not show heat effects consistent with competitive compound binding to the active site. The potent binding affinity observed in the presence of ATP is consistent with the inhibitor design and the proposed Ordered Ter-Ter mechanism for this enzyme; however, the additional binding pathways suggest that the inhibitor can also serve as a product analogue.

Antibacterials designed to target bacterial cell wall biosynthesis accounted for more than 55% of the total antibacterial market in 1998 (*1*). Despite the success in targeting cell wall biosynthesis, there are few antibiotics that target the enzymes involved in the early stages of the biosynthetic pathway, the cytoplasmic production of murein peptidoglycan precursors (Stage I) (*2*). As a result, these enzymes represent a valuable class of targets for the discovery of novel antimicrobial agents. The discovery of novel antibiotics is of increasing importance as bacterial resistance to known antibiotics continues to grow (*3*).

Uridine diphosphate *N*-acetylmuramate:L-alanine ligase (UNAM:Ala ligase or MurC) catalyzes the third chemical step in Phase I of bacterial cell wall biosynthesis. The enzyme is a nonribosomal peptide ligase which utilizes ATP to form an amide bond between L-alanine and UNAM.[1] Mechanistic studies on the *Escherichia coli* MurC enzyme using oxygen isotope analyses (*4*) demonstrated that the enzyme-catalyzed reaction proceeds through an acyl phosphate UNAM intermediate prior to L-alanine addition. Steady-state kinetic and rapid quench studies (*5*) extended these observations and demonstrated that the enzyme follows an Ordered Ter-Ter mechanism where ATP is the first substrate to bind, followed by UNAM and then L-Ala. These studies support a mechanism which is comprised of at least two distinct chemical steps: activation of the UNAM carboxylic acid followed by nucleophilic attack on the acyl phosphate group by L-Ala to result in amide bond formation. The chemical and kinetic mechanism proposed for MurC appears to be conserved among ATP-dependent ligases including other members of the Mur pathway (*6*−*9*), D-Ala-D-Ala ligase (*10*−*13*), and glutamine synthetase (for review see ref *14*). The proposed transition state involves the nucleophilic attack on the acyl phosphate group to generate a tetrahedral intermediate (see Figure 1A). Subsequent release of phosphate or regeneration of the nucleophile results in either amide bond formation or starting materials, respectively.

A number of phosphinate inhibitors have been prepared as transition state mimetics for many of these enzymes (*15*−*25*). Generally, these inhibitors have shown potent inhibition, and several have exhibited slow, tight-binding inhibition properties with near-irreversible potency. Recently, a series of phosphinate inhibitors were prepared as transition state analogues of the MurC-catalyzed reaction (*26*). In this report, we describe the kinetic inhibition properties of one of these analogues (**1**, Figure 1) including time dependence, reversibility, and steady-state kinetic mode of inhibition studies. In addition, we utilized ITC to further evaluate the inhibitor−enzyme binding interactions. Using these techniques, we propose an overall inhibition model which involves several dead-end pathways for multiple enzyme forms. The implications of this model for inhibitor design and drug discovery are discussed.

* To whom correspondence should be addressed. Tel: (781) 839-4531. Fax: (781) 839-4600. E-mail: Stewart.Fisher@AstraZeneca.com.

[‡] Department of Biochemistry and Protein Science.

[§] Current address: Department of Biology, Massachusetts Institute of Technology, 77 Massachusetts Ave., E17-529, Cambridge, MA 02139-4307.

[||] Department of Chemistry.

[⊥] Department of Molecular Sciences.

[1] Abbreviations: AMP-PCP, β,γ-methyleneadenosine 5′-triphosphate; EP-GlcNAc, enolpyruvate−*N*-acetylglucosamine; ITC, isothermal titration calorimetry; PEP, phosphoenolpyruvate; RP-HPLC, reverse-phase high-performance liquid chromatography; UDP-GlcNAc, uridine diphosphate−*N*-acetylglucosamine; UNAM, uridine diphosphate−*N*-acetylmuramic acid; UNAM-Ala, uridine diphosphate−*N*-acetylmuramyl-L-alanine.

10.1021/bi015567m CCC: $20.00
Published on Web 09/13/2001

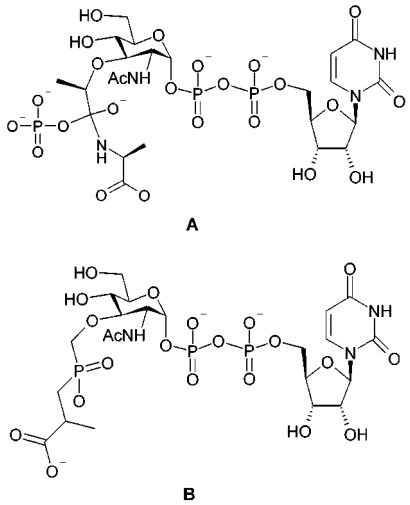

FIGURE 1: (A) Proposed reaction transition state comprised of the tetrahedral carbon center and (B) phosphinate inhibitor **1**.

MATERIALS AND METHODS

Reagents. Malachite green hydrochloride and $MgCl_2$ were purchased from J. T. Baker. AMP-PCP was obtained from Roche and Triton X-100 from Fisher Scientific. All other reagents were purchased from Sigma. Ammonium molybdate−malachite green reagent was prepared as described (*27*) without the use of Sterox and where glass was replaced by plastic containers. The inhibitor was prepared as described (*26*).

Enzymatic Synthesis and Purification of UNAM. UNAM was prepared using a two-step enzymatic process. To obtain 3 g of UNAM, a reaction mixture (225 mL) containing 66.7 mM Tris-HCl, pH 8.0, 26.7 mM KCl, 26.0 mM UDP-GlcNAc, 26.0 mM NADPH, 112.3 mM PEP, and 43.2 mM DTT was slowly brought to pH 8.0 with 5 N NaOH. An aliquot of *E. coli* MurA (4 mL, 1.41 mg/mL) was added with stirring in the dark at room temperature. The reaction was monitored by analytical RP-HPLC using isocratic conditions of 50 mM ammonium formate, pH 3.7, with a C_{18} ODS-AQ S-5 120 Å 4.6 × 250 mm column from YMC (Waters). All samples were brought to pH 3.7 and mixed prior to injection on the column, and the chromatogram was monitored at 254 nm. Additional MurA was added until conversion of UDP-GlcNAc to EP-GlcNAc was complete. An aliquot of *E. coli* MurB (4 mL, 2.99 mg/mL), along with fresh DTT and NADPH, was then added, after the pH was adjusted to 8.0. Additional MurB, DTT, and NADPH were added until greater than 85% yield of UNAM was achieved as assessed by RP-HPLC. Purification of the product was performed using RP-HPLC on a C_{18} ODS-AQ S-10P 120 Å 50 × 250 mm column under isocratic conditions (100 mM ammonium formate, pH 3.7). The purified fractions were pooled and concentrated under reduced pressure, then repeatedly diluted with doubly distilled H_2O, and concentrated under reduced pressure to remove volatile salt contaminants. The UNAM concentration was assessed using UV spectroscopy at 262 nm as reported (*28*). The synthesis of UNAM-Ala was performed as reported (*28*) but was also purified by HPLC as described above.

Overexpression and Purification of E. coli MurC. The *murC* gene was cloned from the chromosomal DNA of wild-type *E. coli* strain DH5α using the polymerase chain reaction. Amplification was performed using PCR supermix (GIBCO BRL) and the following primers: 5′-GCGCAATTCCATATGAATACACAACAATTGGCA-3′ and 5′-GCGCAACTCGAGTCAGTCATGTTGTTCTTCCTC-3′ (*Nde*I and *Xho*I sites underlined). The PCR product was purified using a Centriflex Gel Filtration Cartridge (Advanced Genetic Technologies Corp.) and digested with *Nde*I and *Xho*I. The resulting fragment was then purified and ligated into the *Nde*I- and *Xho*I-digested expression vector pET23a (Novagen), producing the plasmid pET23a-*murC*. The DNA sequence of the cloned *murC* was confirmed by sequencing on an ABI PRISM 377 DNA sequencer (Perkin-Elmer) using an ABI PRISM Dye Terminator Cycle Sequencing Ready Reaction Kit with AmpliTaq DNA polymerase (Perkin-Elmer). Computer analysis of DNA sequences was performed with Sequencher (Gene Codes Corp.) and with Genetics Computer Group programs (*29*). For protein overproduction, the plasmid was transformed into BL21(DE3) (Novagen) and plated on LB containing 50 μg/mL ampicillin at 37 °C overnight. A single colony of BL21(DE3)/pET23a-*murC* was inoculated into a 50 mL culture of LB containing 50 μg/mL ampicillin and grown overnight. Samples (3 × 10 mL) of the overnight culture were added to 3 × 1 L of LB containing 50 μg/mL ampicillin and grown at 37 °C with aeration for 3 h to reach mid-logarithmic phase (OD_{600} = 0.6), and then IPTG was added to a final concentration in each culture of 1 mM. After 3 h induction, the cells were harvested by centrifugation at 5000*g* for 10 min at 4 °C. The cell pellets were washed with 300 mL of 20 mM Tris-HCl, pH 7.5, and centrifuged again (5000*g*, 10 min) at 4 °C. Cell paste was stored at −20 °C and protein expression checked by SDS−PAGE. The frozen cell paste (5.81 g from 3 L of culture) was resuspended in 100 mL of lysis buffer [20 mM Tris-HCl, pH 7.5, 2.5 mM DTT, 1 mM EDTA, 1 mM PMSF, and 2 protease inhibitor cocktail tablets (Roche Molecular Biochemical)]. Cells were lysed by a French press (2 × 18 000 psi), and the resulting effluent was centrifuged at 30 000 rpm for 30 min at 4 °C. The supernatant was loaded at a flow rate of 1 mL/min onto a Q-Sepharose HP (HR10/10) column (Pharmacia) preequilibrated with buffer A (20 mM Tris-HCl, pH 7.5, 1 mM EDTA, and 2.5 mM DTT). The column was then washed with buffer A, and the protein was eluted by a linear gradient from 0 to 1 M NaCl in buffer A. Active protein was identified at 150 mM NaCl. Fractions containing active protein were pooled, and $(NH_4)_2SO_4$ was added to give a final concentration of 1 M and loaded onto a phenyl-Sepharose HP (HR10/10) column (Pharmacia) preequilibrated with 1 M $(NH_4)_2SO_4$ in buffer A at a flow rate of 1 mL/min. After being washed with 1 M $(NH_4)_2SO_4$ in buffer A, the protein was eluted using a linear gradient from 1 to 0 M $(NH_4)_2SO_4$ in buffer A. Fractions containing active protein were found to elute at 0.45 M $(NH_4)_2SO_4$ and were pooled and dialyzed (1:100) at 4 °C for 6 h against buffer B (20 mM Tris-HCl, pH 7.5, 2.5 mM DTT, 10 mM $MgCl_2$, 150 mM NaCl, and 500 μM ATP), followed by an overnight dialysis (1:50) against buffer B containing 20% glycerol. The protein was characterized by SDS−PAGE analysis and analytical LC-MS (expected MW = 53 674.1 Da, observed = 53 673.0 Da) and judged to be at >95% purity. The protein was stored at −80 °C.

Activity Assay Using Malachite Green Phosphate Detection. Enzyme activity was measured using a 96-well micro-

titer-format, discontinuous assay of inorganic phosphate production. For inhibition studies, the enzyme was usually preincubated for 20 min with the inhibitor; control reactions utilized water or DMSO. Reactions were initiated by the addition of substrates and then quenched after 20 min with the addition of ammonium molybdate−malachite green reagent in 1 N HCl at 1.5 times the assay volume. Absorbance (650 nM) was read 5 min after the quench. The final concentrations of components in a typical assay were 50 mM Tris-HCl, pH 8.0, 2.5 mM DTT, 10 mM $MgCl_2$, 0.01% (w/v) Triton X-100, and 0.33 μg/mL (6.2 nM) *E. coli* MurC (assay buffer). Absorbance values were converted to concentrations using standard curves prepared under identical conditions (without enzyme) using KH_2PO_4 additions ranging over 0−1.8 nmol of phosphate (0−30 μM final).

Steady-State Kinetic Analyses. The malachite green assay was used for all kinetic measurements as described above. Determination of $K_{M,app}$ for each substrate was performed under moderately saturating conditions of the other two substrates as follows: [ATP] = 200 μM, [UNAM] = 200 μM, and [L-Ala] = 500 μM. The nomenclature for all steady-state kinetic analyses is that of Cleland. Full kinetic characterization was performed by collecting initial velocity data for a 7 × 6 × 6 matrix of substrate concentrations (ATP, UNAM, and Ala, respectively), where each substrate was varied from 0.25 to 5 × $K_{M,app}$. All data were taken in quadruplicate and averaged, and standard error values were calculated for all substrate concentrations prior to nonlinear regression analysis. Nonlinear regression analysis was performed with GraFit 4.0 (*30*). The data were fit using nonlinear regression analysis according to the steady-state equations for Ter reactant systems (*31*). Data fitting was initiated using a matrix of estimated values for each parameter. Experimental standard error values were employed in the data fitting routines.

Determination of K_I for AMP-PCP. AMP-PCP was varied (0−500 μM) against ATP (0−475 μM) with fixed concentrations of L-alanine ([L-Ala] = 275 μM) and UNAM ([UNAM] = 100 μM). Reciprocal plots of the data intersected on the *Y*-axis, consistent with competitive inhibition with respect to ATP. The K_I of AMP-PCP was determined through a slope replot analysis.

Inhibition Property Assessment. Inhibitory properties of **1** were surveyed under routine conditions where the final concentrations of substrates were as follows: 300 μM ATP, 50 μM L-alanine, and 75 μM UNAM. For dose−response analysis, the inhibitory effect on enzyme activity was measured over a 10 point, serial dilution (1:2) of inhibitor (6−3120 nM final). The inhibitory effect was calculated as a percentage of full activity from control reactions and fitted using nonlinear regressions to the Hill equation to yield the concentration required for 50% inhibition (IC_{50} value). For time dependence studies, a stock solution of enzyme in assay buffer containing 0.66 μg/mL (12.4 nM) MurC was prepared. The stock was evenly divided into three aliquots, and for one of the solutions 150 nM inhibitor was added, to another 150 nM inhibitor plus 1 mM ATP, and the last solution was used as a control. Enzymatic activity of the stocks was monitored over time by dilution (1:2) of samples with buffer or with buffer containing 150 nM inhibitor. The final concentrations in the assay well for substrates were 300 μM ATP, 100 μM UNAM, and 100 μM L-alanine. Reversibility of inhibition was tested using a comparative dilution analysis. In these experiments, two aliquots each containing high concentrations of enzyme (16 nM, 20-fold) and inhibitor (150 nM) were prepared and incubated for 30 min. After preincubation the samples were then diluted either with buffer or with buffer containing 150 nM inhibitor, and the reactions were initiated and analyzed as above with substrates held at 300 μM ATP, 100 μM UNAM, and 100 μM L-alanine.

Phosphorylation of Inhibitor. To assess whether the inhibitor undergoes phosphorylation by the enzyme, high concentrations of inhibitor (100 μM), enzyme (30 μM), and ATP (325 μM) were incubated in reaction buffer at room temperature for 20 min, then heated to 100 °C (5 min), chilled on ice (30 min), and centrifuged (10 min, 14000*g*). Aliquots of the reaction mixture (10 μL) were diluted with water (40 μL), quenched with malachite green reagent (75 μL), and measured at 650 nm. Results from these experiments were compared to control reactions measured under identical conditions except with the inhibitor omitted.

Mode of Inhibition Studies of E. coli MurC with Inhibitor. From the dose−response analysis of **1** (IC_{50} = 42 nM), a 7 × 8 matrix was created where the inhibitor was varied from 0.3 to 6 × IC_{50} for each substrate (0.3−6 × $K_{M,app}$) while the remaining two substrates remained constant. The concentrations of the fixed substrates were as follows: [ATP] = 240 μM, [UNAM] = 75 μM, [Ala] = 50 μM (subsaturating); [ATP] = 600 μM, [UNAM] = 150 μM (saturating). Initial velocity data were collected in triplicate and averaged. Linear least-squares fits were performed for each inhibitor concentration in reciprocal space and qualitatively analyzed for inhibition characteristics with respect to each substrate (competitive, mixed, and uncompetitive). In addition, global fit analyses according to the full velocity equation (Scheme 2) were performed as described above. Goodness of fit was assessed by evaluation of fitted curve residuals (χ^2) and comparison of kinetic constant values obtained from the inhibition model with that obtained from the substrate order of addition steady-state studies.

Isothermal Titration Calorimetry. Samples of enzyme for titrations were prepared by extensive dialysis (three changes at 1:1000 dilution each) against the reaction buffer (50 mM Tris-HCl, pH 8.0, 2.5 mM $MgCl_2$, and 1 mM TCEP) and substrates/products as required. Final enzyme concentrations were confirmed by UV spectroscopy, and ligand solutions were prepared by dilution of a concentrated stock (≈10 mM) into the reserved final dialysate buffer. Samples were degassed by vacuum aspiration for 10 min prior to loading, and all titrations were performed at 25 °C. In most cases, more than 40 injections were performed for each thermogram, and the final molar ratio of ligand to enzyme was >3.0. In all cases, reserved dialysate buffer was used in the reference cell. Titrations were performed on a Microcal VP-ITC, and all analysis of thermograms was performed using the Origin 5.0 package supplied with the instrument. Normalization of enzyme thermograms was usually performed by subtraction of heats obtained from ligand dilution experiments performed under conditions in the absence of enzyme. In some cases, the heats of dilution were obtained by extrapolation of high molar ratio injections and subsequently subtracted from the entire thermogram. Comparative analysis of the heat of dilution normalization methods indicated that differences between the two methods were

Scheme 1: Steady-State Equation for Ordered Ter-Ter Kinetic Model

$$\frac{v}{V_{max}} = \frac{[A][B][C]}{K_{ia}K_{ib}K_{m_C} + K_{ib}K_{m_C}[A] + K_{ia}K_{m_B}[C] + K_{m_C}[A][B] + K_{m_B}[A][C] + K_{m_A}[B][C] + [A][B][C]}$$

Table 1: Ordered Ter-Ter Steady-State Kinetic Parameters Obtained from Global Fit Analyses

parameter	value
k_{cat}	404 ± 33.4 min^{-1}
$K_{M,ATP}$	18.4 ± 6.43 μM
$K_{M,UNAM}$	35.5 ± 5.22 μM
$K_{M,Ala}$	20.7 ± 5.26 μM
$K_{I,ATP}$	145 ± 18.5 μM
$K_{I,UNAM}$	117 ± 35.4 μM

below experimental noise. Thermograms were then integrated and fit using nonlinear regression curve fitting to a single binding site model to provide ΔH, K_d, and the binding stoichiometry (n). Initial optimization of titration conditions revealed that moderately high enzyme concentrations (>5 μM) were required for accurate binding thermograms. However, enzyme solubility at high concentrations (>25 μM) was sensitive to the total nucleotide concentration (>10 mM), including ATP, ADP, UNAM, and inhibitor. This solubility limitation resulted in nonreproducible and erratic binding isotherms. Optimal conditions were observed with enzyme concentration at or below 8 μM; at these concentrations reproducible thermograms were observed at total nucleotide concentrations sufficient for complete saturation of the enzyme (>1 mM) where desired.

RESULTS

Enzyme Characterization. Preliminary characterization of the enzyme was performed by measuring apparent K_M values for each substrate under moderately saturating concentrations of the other two substrates. Under these conditions, the apparent K_M for ATP was 61.4 ± 4.63 μM, for L-alanine was 56 ± 0.58 μM, and for UNAM was 19.20 ± 12.6 μM. In general, these data are generally consistent with published values, with the exception of the K_M value obtained for ATP, which is significantly lower in our studies (*32*, *33*). The discrepancy in values may be due to differences in enzyme activity assay format since the biophysical characterization of the enzyme (pH optimum, salt dependence, and stability; data not shown) was consistent with the properties reported for this enzyme (*33*). Using these data, a $7 \times 6 \times 6$ matrix of substrate concentrations was prepared, where each substrate was varied over a range corresponding to $0.25-5 \times K_{M,app.}$ Initial rate data collected for this matrix of substrate concentrations were fit using nonlinear regression analysis according to the equation for an Ordered Ter-Ter mechanism. The data were fit to several other Ter reactant systems including Hexa-Uni-Uni, Bi-Uni-Uni-Bi, and Uni-Uni-Bi-Bi; however, the best fit for the data was to the Ordered Ter-Ter mechanism forward velocity equation (see Scheme 1). These results are consistent with previous studies which demonstrated the following substrate addition order: ATP, UNAM, and Ala (*34*). The kinetic constants obtained from the fit are shown in Table 1. On the basis of these results the calculated $K_{M,app}$ values for each substrate corresponding to the conditions used in these studies are as follows: $K_{M,app,ATP} = 47$ μM, $K_{M,app,UNAM} = 69$ μM, and $K_{M,app,Ala} = 41$ μM. These results are in good agreement with the experimentally measured values, thereby lending support to the overall global analysis, with the exception of $K_{M,app,UNAM}$. We noted that this substrate exhibited mild substrate inhibition at high substrate concentrations (>125 μM), which would be expected to result in an underestimate of the $K_{M,app,UNAM}$ from the velocity curve obtained under conditions of saturating [ATP] and [L-Ala].

Inhibition Properties of the Phosphinate Inhibitor. The inhibition properties of **1** were initially surveyed using conditions suitable for screening. Dose−response curves generated under these conditions demonstrated potent inhibition of the enzyme ($IC_{50} = 42 \pm 1.0$ nM). The time dependence of inhibition was evaluated by varying the enzyme−inhibitor incubation time prior to reaction initiation; the inhibition remained constant over the time period tested (2 min−8 h). Further, the effect of substrates in the preincubation conditions was analyzed; addition of ATP, AMP-PCP, and/or UNAM had no effect on the time dependence ($t = 30$ min, 8 h) or potency of inhibition. Reversibility of inhibition was assessed using a comparative dilution analysis. The inhibition of **1** was fully reversible upon dilution, suggesting that the enzyme−inhibitor binding interactions occur through noncovalent bonds and that the enzyme−inhibitor complex dissociation rates are fast relative to this experimental time scale. In support of these findings, no covalent adducts were identified on the protein after inhibitor incubation by electrospray mass spectral analysis.

Phosphorylation of phosphinate-based transition state inhibitors has been observed in a number of systems including those designed for D-Ala-D-Ala ligase (*15*, *20*, *21*) and glutamine synthetase (*18*, *24*, *25*). Phosphorylation of **1** was analyzed spectrophotometrically under conditions where sufficient enzyme, ATP, and inhibitor were incubated to initiate phosphate transfer. Subsequent brief exposure to heat has been shown to hydrolyze phosphoryl phosphinate intermediates, resulting in inorganic phosphate and the intact inhibitor (*15*, *20*). The conditions employed in these studies were suitable for detection of substoichiometric phosphate transfer levels using the malachite green assay. Under these conditions no excess phosphate was detected above that detected in control reactions run in the absence of inhibitor. On the basis of the detection limits of the assay, <10% of the inhibitor was phosphorylated by the enzyme. In sum, these results strongly suggest that inhibitor phosphorylation is not a significant event in the inhibition pathway.

Steady-State Mode of Inhibition Studies. On the basis of the steady-state kinetic enzyme mechanism (Ordered Ter-Ter) and the observed inhibition properties (fully reversible, time independent), a single reversible, dead-end inhibition model was proposed (see Figure 2). In this case, the inhibitor is expected to bind exclusively to the [E−ATP] form. The equation solved for this model (see Scheme 2) predicts that the inhibitor exhibits uncompetitive inhibition with respect to ATP, competitive inhibition with respect to UNAM, and mixed-type inhibition with respect to alanine when the other

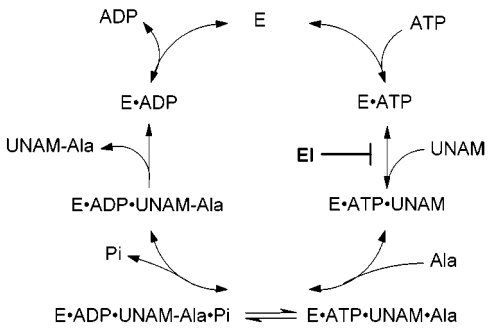

FIGURE 2: Proposed mode of inhibition model based on inhibitor design.

respective substrates were held at saturating concentrations. However, mixed-type inhibition was observed with respect to all three substrates as shown in Figure 3. In these studies, fixed concentrations for ATP and UNAM were kept at moderately saturating concentrations ($5 \times K_{M,app}$) to minimize assay interference problems, but concerns arose that these concentrations would not be sufficient to fully saturate the enzyme and produce clean kinetic profiles. To this end, kinetic measurements taken at higher ATP and UNAM concentrations ($10 \times K_{M,app}$), while not as precise, were qualitatively similar to those in Figure 3. Finally, global fit analyses were performed on the inhibition data sets according to the equation solved for this model (Scheme 2); in all cases extremely poor fits were obtained regardless of initial estimate settings and variation of the convergence criteria (data not shown). These results suggest that the phosphinate inhibitor binds to multiple forms of the enzyme.

Isothermal Titration Calorimetry. ITC was used to evaluate whether **1** bound to multiple forms of the enzyme. In these studies, the conditions for the titrations were designed to closely match those used in the kinetic analyses; however, it was found that substantially more enyzme was required to generate sufficient binding heats. In general, the increased enzyme concentration was not expected to affect the interpretation of binding results as the enzyme kinetics remain linear at these concentrations (*33*). However, it was noted that conditions of combined high enzyme and high nucleotide concentrations ([nucleotide] > mM) induced protein insolubility, which resulted in spurious titration thermograms. This problem was alleviated by reducing the enzyme concentration ([MurC] < 8 μM).

Titrations of **1** with the enzyme were performed under a number of conditions, and the results are summarized in Table 2. The most surprising result was obtained with enzyme in the absence of substrates; a clear binding thermogram was obtained under this condition (see Figure 4A). While the K_d obtained from fitting these data is relatively high compared to the observed dose−response inhibition potency, it is clear that the observed potency is sufficient to represent an active dead-end inhibition mode under steady-state conditions. These results are consistent with the mixed mode of inhibition observed when ATP was the varied substrate. However, the observed binding under this condition is not consistent with the Ordered Ter-Ter mechanism proposed for this enzyme, which would predict that binding of a UNAM mimic would require ATP binding. Indeed, titrations of the enzyme with the inhibitor in the presence of saturating ATP demonstrated potent binding (see Figure 4B). These results strongly suggest that the inhibitor binds to the enzyme as designed and that this binding mode represents the lowest energy dead-end pathway.

Titrations performed under conditions of high ADP concentrations revealed that the inhibitor can also bind to the enzyme−product complex with reasonable potency (see Figure 4C). This result, while not particularly surprising, highlights another complicating feature of the steady-state mode of inhibition analyses. The K_d obtained from fitting these data suggests that this complex may form at low, but detectable levels under the conditions employed in the steady-state analyses, even though care was taken to measure rates under initial conditions (<10% of product formed). These data suggest that models proposed for fitting the steady-state mode of inhibition data should not be derived from rate equations containing only terms for the forward direction but rather utilize the complete steady-state equation. These results also clearly demonstrate that the γ-phosphate of ATP is not required for tight binding of the inhibitor to the enzyme; only a 5-fold loss of binding is observed with ADP relative to ATP. To this end, the effect of AMP-PCP, a non-hydrolyzable ATP analogue, on binding was assessed. This analogue was shown to be a competitive inhibitor of the enzyme with respect to ATP ($K_I = 27.6 \pm 10.3$ μM). Titrations carried out under saturating AMP-PCP exhibited moderate binding of the inhibitor to the enzyme. Taken together, the titrations with ADP and AMP-PCP support the conclusion that phosphorylation of **1** is not required for potent binding to the enzyme.

Finally, no heat of binding was observed under conditions of saturating ATP and UNAM. It is possible that binding occurs under this condition that is driven by purely entropic factors and therefore would not be detected by ITC under the conditions used in this study. However, we consider this situation unlikely and believe that these data suggest that the inhibitor binds as designed to the UNAM site and that the natural substrate can compete for binding at saturating concentrations. In summary, three binding modes were identified using ITC, and the overall binding model is shown in Figure 5.

DISCUSSION

The Mur ligases represent a valuable class of enzyme targets for the discovery of novel antibiotic agents. Recently, these enzymes have been classified as a distinct ligase superfamily using structural (*6*, *35*−*37*) and genomic (*9*, *38*) comparisons to other known ADP-dependent ligases. The results summarized in Table 2 indicate that **1** is a potent inhibitor of *E. coli* MurC with an affinity in the nanomolar range. To our knowledge, this is the most potent inhibitor reported for MurC and is comparable to the most potent inhibitors reported to date for the entire Mur ligase superfamily (*19*, *22*, *23*, *39*). Through detailed binding analysis, it was shown that the inhibitor binds to a number of enzyme forms with varying, but significant, potencies. The multiple dead-end pathways exhibited by the inhibitor were unexpected, and the complex binding model in Figure 5 suggests that the inhibitor is more than a simple transition state analogue. At a basic level, to the extent that the inhibitor actually mimics the transition state when bound in the presence of ATP, it is possible that the inhibitor could be

Scheme 2: Steady-State Equation for Proposed Mode of Inhibition Model

$$\frac{v}{V_{max}} = \frac{[A][B][C]}{K_{ia}K_{ib}K_{m_C} + K_{ib}K_{m_C}[A] + K_{ia}K_{m_B}[C] + K_{m_C}[A][B] + K_{m_B}[A][C] + K_{m_A}[B][C] + [A][B][C] + \frac{[I][A]}{K_I}\left(K_{ib}K_{m_C} + K_{m_B}[C]\right)}$$

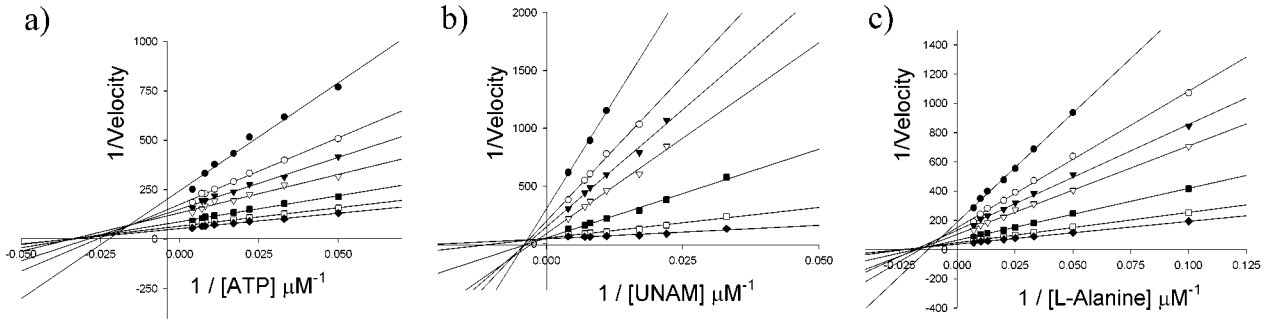

FIGURE 3: Reciprocal plot of steady-state inhibition data collected for **1** versus (a) ATP ([UNAM] = 75 μM, [L-Ala] = 50 μM), (b) UNAM ([ATP] = 240 μM, [L-Ala] = 50 μM), and (c) L-Ala ([ATP] = 240 μM, [UNAM] = 75 μM).

Table 2: Thermodynamic Values Determined from Isothermal Titration Calorimetric Measurements

condition	K_d (μM)[a]	n[a]	$-\Delta H$ (kcal/mol)[a]
MurC	1.80−2.79	1.16−1.24	8.15−8.90
MurC, ATP	0.0969−0.108	0.749−0.806	4.81−5.41
MurC, ATP, UNAM	ND[b]	ND	ND
MurC, ADP	0.371−0.751	0.723−0.824	5.64−7.01
MurC, AMP-PCP	0.784−1.30	0.854−0.945	5.02−5.76

[a] Data represent 95% confidence intervals for the best fitted curve through the experimental data set. Results from multiple data sets were within these intervals. [b] No heat of binding was observed.

serving as a simple multisubstrate analogue (for review see ref *40*). Arguments using the simple magnitude of inhibition as evidence for transition state mimicry must be tempered by the prediction that multisubstrate analogues have the potential to bind up to 10^8-fold more tightly than the corresponding substrates alone. There is precedent that phosphinate mimics can serve as effective transition state analogues of peptidase reactions (*41*) and in enzyme-catalyzed ligation reactions where the inhibitors undergo phosphorylation (*10*, *15*−*17*). However, it is not clear that incorporation of the tetrahedral phosphinate center, without subsequent phosphorylation, is sufficient to mimic the peptide ligation transition state in the MurC-catalyzed reaction. The data in this report cannot be used to conclusively demonstrate whether **1** acts as a transition state analogue or a simple multisubstrate analogue of MurC. Further characterization of the enzyme mechanism, including determination of the rate limiting step, along with inhibition studies on appropriate enzyme mutants may support transition state analogue designation. Alternatively, structural studies can support analysis of the factors that stabilize the transition state and the extent that an inhibitor utilizes these interactions for potent binding. Unfortunately, even though a number of crystal structures have been obtained for MurD, MurE, and MurF, no structures have been reported which contain transition state-based inhibitors. Such a structure would be extremely useful in comparing and evaluating the transition state binding determinants within the Mur ligase enzyme active site with those identified for other structurally defined ATP-dependent ligases complexed with phosphinate inhibitors (*12*, *17*).

The additional dead-end pathways exhibited by the inhibitor may be attributed to features of the inhibitor design or the resemblance between **1** and the product UNAM-Ala. In terms of inhibitor design, the preparation of the inhibitor used in this study was a mixture of diastereomers at the alanyl-derived stereo center. It is formally possible that different kinetic forms of enzyme can bind the diastereomers of the inhibitor to result in the multiple inhibition pathways. This hypothesis was discounted on the basis of the exquisite substrate stereoselectivity reported for this enzyme (*5*), and the results from ITC experiments support a single binding mode with the correct binding stoichiometry for single diastereomer binding. It was considered more likely that the additional dead-end pathways were due to the resemblance of the inhibitor to the reaction product UNAM-Ala. Product inhibition studies with UNAM-Ala demonstrated that it is a mixed-type inhibitor for all three substrates and is therefore also predicted to form multiple dead-end pathways, potentially including one with enzyme alone (*34*). Due to the mixed mode of action exhibited by UNAM-Ala, it is not possible to obtain a meaningful product inhibition constant from the kinetic data. Similarly, attempts to measure the UNAM-Ala binding affinity using ITC were unsuccessful due to poor protein solubility at the high nucleotide concentrations required for affinity measurements. These experimental difficulties preclude a quantitative comparison of the inhibitor and UNAM-Ala binding affinities, but the overall inhibition properties of **1** suggest that the inhibitor may act as a product analogue, particularly for the weaker affinity interactions.

The impressive inhibition profile exhibited by **1** is a valuable attribute in the discovery of antimicrobial agents; however, further development of this would be expected to be difficult based on physicochemical and pharmacokinetic properties considerations (e.g., molecular weight, permeability and metabolic liability) (*42*). One strategy for further optimization would be to identify and further improve

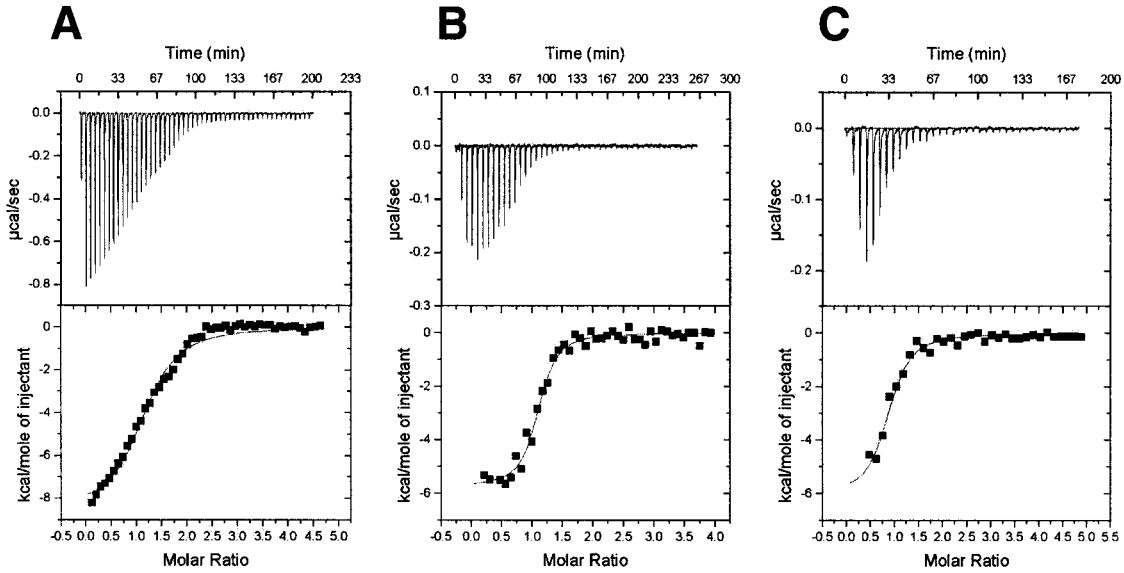

FIGURE 4: Representative data from isothermal titration calorimetry experiments performed with the inhibitor (syringe) and (A) MurC, (B) MurC with ATP ([ATP] = 400 μM), and (C) MurC with ADP ([ADP] = 400 μM) in the reaction cell.

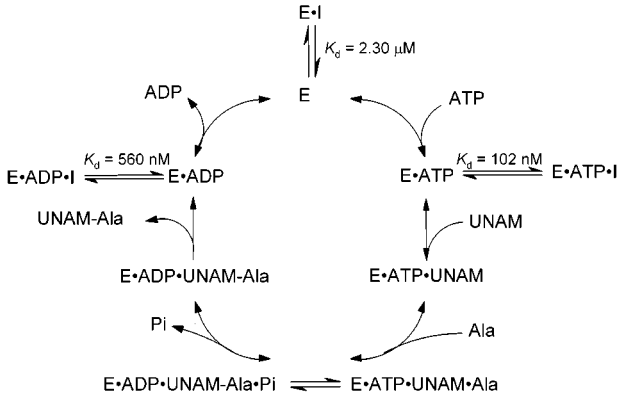

FIGURE 5: Schematic representation of the observed modes of inhibition by phosphinate inhibitor **1** (K_d values represent the mean value obtained from fitted curves of calorimetric thermograms).

interactions/mechanisms responsible for potent inhibition concomitant with reduction of the issues regarding the overall physicochemical properties. This approach could benefit from the properties exhibited by the phosphinate transition state analogues designed for other ATP-dependent ligases including glutamine synthetase (*18*, *24*, *25*) and D-Ala-D-Ala ligase (*15*, *17*, *20*, *21*). In these two examples, the inhibitors exhibit time-dependent, near-irreversible binding. Mechanistic studies have shown that the inhibition pathway follows a two-step process where the inhibitor first binds reversibly with weak affinity but forms a slow, tight-binding complex with the enzyme after phosphorylation of the inhibitor to form an acyl phosphate intermediate. Based on this precedent, it is surprising that **1** exhibits time-independent, fully reversible inhibition. Further, no phosphorylation of the inhibitor was observed under conditions of saturating ATP and inhibitor. These observations demonstrate that phosphorylation of **1** is not required for potent inhibition and raise the question of whether MurC can phosphorylate the bound inhibitor. Comparative analysis of the inhibitor with the proposed reaction transition state illustrates that while many of the key interactions have been accommodated by the inhibitor design, the inhibitor differs from the parent substrate structures. These differences are expected to have subtle, but potentially important, effects on the overall inhibitor geometry and electronic properties, and it is possible that these effects render the inhibitor inactive to phosphorylation. This question can be extended to other members of the Mur family where phosphinate inhibitors have been prepared and studied; no evidence has been reported for phosphorylation of phosphinate inhibitors targeted to MurD (*19*, *22*) and MurE (*23*). In this context, the different phosphinate inhibitor phoshorylation reactivities observed between the Mur ligases and other ATP-dependent ligases may indicate that there are fundamental differences between the enzymes rather than the inhibitor design. Despite the fact that the Mur ligases share a similar chemical mechanism and quaternary structural organization comprised of three domains with other ATP ligases, none of the individual domains show significant similarity outside of the Mur ligase superfamily. These observations suggest that the tertiary structures of the individual domains, and hence the active sites of the Mur ligases, are highly optimized to process the cognate substrates and that relatively small changes to the natural substrates are not easily accommodated within the chemical framework of the active site.

The multiple binding modes observed with this inhibitor have additional important implications for drug discovery. Structure−activity relationships (SAR) derived from screening a series of related inhibitors assume that observed binding affinity changes are due to altered interactions with the enzyme, but these studies do not provide information regarding the dead-end pathway responsible for the most potent binding interaction. However, if the dominant binding mode changes with inhibitor modification, the resulting SAR can become confusing or uninterpretable. This concern has to be countered with the need for rapid, high-volume potency assessment requirements of the drug discovery process. Clearly, a balance must be made between efficient analogue testing and detailed analysis of select inhibitors to ensure that the SAR is tracking with the assumed binding mode. A more subtle potential benefit from regular detailed analysis of inhibitor binding involves those cases where changes in inhibitors improve the binding affinities in secondary (weaker) binding

modes, but the dominant binding mode potency remains unchanged. The absolute potency of inhibitor binding, determined through routine analogue testing, would mask these secondary improvements. In this situation, improvements to the secondary modes are potential "missed opportunities"; intelligent application of this detailed SAR would utilize these improvements in future designs to maximize potency among multiple binding modes.

ACKNOWLEDGMENT

We thank G. Deng for N-terminal sequencing and mass spectrometry analyses, O. Rivin for amino acid analyses, and K. MacCormack for DNA sequencing.

REFERENCES

1. Ireland, S. (1999) Decision Resources, Inc., Waltham, MA.
2. Wong, K. K., and Pompliano, D. L. (1998) *Adv. Exp. Med. Biol. 456*, 197−217.
3. Walsh, C. T. (2000) *Nature 406*, 775−781.
4. Falk, P. J., Ervin, K. M., Volk, K. S., and Ho, H. T. (1996) *Biochemistry 35*, 1417−1422.
5. Emanuele, J. J., Jr., Jin, H., Jacobson, B. L., Chang, C. Y., Einspahr, H. M., and Villafranca, J. J. (1996) *Protein Sci. 5*, 2566−2574.
6. Bertrand, J. A., Auger, G., Martin, L., Fanchon, E., Blanot, D., Le Beller, D., van Heijenoort, J., and Dideborg, O. (1999) *J. Mol. Biol. 289*, 579−590.
7. Vaganay, S., Tanner, M. E., van Heijenoort, J., and Blanot, D. (1996) *Microb. Drug Resist. 2*, 51−54.
8. Anderson, M. S., Eveland, S. S., Onishi, H. R., and Pompliano, D. L. (1996) *Biochemistry 35*, 16264−16269.
9. Eveland, S. S., Pompliano, D. L., and Anderson, M. S. (1997) *Biochemistry 36*, 6223−6229.
10. Mullins, L. S., Zawadzke, L. E., Walsh, C. T., and Raushel, F. M. (1990) *J. Biol. Chem. 265*, 8993−8998.
11. Shi, Y., and Walsh, C. T. (1995) *Biochemistry 34*, 2768−2776.
12. Fan, C., Moews, P. C., Walsh, C. T., and Knox, J. R. (1994) *Science 266*, 439−443.
13. Wright, G. D., and Walsh, C. T. (1992) *Acc. Chem. Res. 25*, 468−473.
14. Eisenberg, D., Gill, H. S., Pfluegl, G. M. U., and Rotstein, S. H. (2000) *Biochim. Biophys. Acta 1477*, 122−145.
15. Duncan, K., and Walsh, C. T. (1988) *Biochemistry 27*, 3709−3714.
16. Ellsworth, B. A., Tom, N. J., and Bartlett, P. A. (1996) *Chem. Biol. 3*, 37−44.
17. Fan, C., Park, I. S., Walsh, C. T., and Knox, J. R. (1997) *Biochemistry 36*, 2531−2538.
18. Farrington, G. K., Kumar, A., and Wedler, F. C. (1987) *J. Med. Chem. 30*, 2062−2067.
19. Gegnas, L. D., Waddell, S. T., Chabin, R. M., Reddy, S., and Wong, K. K. (1998) *Bioorg. Med. Chem. Lett. 8*, 1643−1648.
20. McDermott, A. E., Creuzet, F., Griffin, R. G., Zawadzke, L. E., Ye, Q. Z., and Walsh, C. T. (1990) *Biochemistry 29*, 5767−5775.
21. Parsons, W. H., Patchett, A. A., Bull, H. G., Schoen, W. R., Taub, D., Davidson, J., Combs, P. L., Springer, J. P., Gadebusch, H., Weissberger, B., et al. (1988) *J. Med. Chem. 31*, 1772−1778.
22. Tanner, M. E., Vaganay, S., van Heijenoort, J., and Blanot, D. (1996) *J. Org. Chem. 61*, 1756−1760.
23. Zeng, B., Wong, K. K., Pompliano, D. L., Reddy, S., and Tanner, M. E. (1998) *J. Org. Chem. 63*, 10081−10086.
24. Logush, E. W., Walker, D. M., McDonald, J. F., and Franz, J. E. (1990) *Biochemistry 29*, 366−372.
25. Johnson, C. R., Boettcher, B. R., Cherpeck, R. E., and Dolson, M. G. (1990) *Bioorg. Chem. 18*, 154−159.
26. Reck, F., Marmor, S., Fisher, S. L., and Wuonola, M. A. (2001) *Bioorg. Med. Chem. Lett. 11*, 1451−1454.
27. Lanzetta, P. A., Alvarez, L. J., Reinach, P. S., and Candia, O. A. (1979) *Anal. Biochem. 100*, 95−97.
28. Reddy, S. G., Waddell, S. T., Kuo, D. W., Wong, K. W., and Pompliano, D. L. (1999) *J. Am. Chem. Soc. 121*, 1175−1178.
29. Devereux, J., Haeberli, P., and Smithies, O. (1984) *Nucleic Acids Res. 12*, 387−395.
30. Leatherbarrow, R. J. (1998) *Grafit Version 4.0*, Erithacus Software Ltd., Staines, U.K.
31. Segel, I. H. (1993) *Enzyme Kinetics*, John Wiley & Sons, New York, NY.
32. Liger, D., Masson, A., Blanot, D., van Heijenoort, J., and Parquet, C. (1996) *Microb. Drug Resist. 2*, 25−27.
33. Jin, H., Emanuele, J. J., Jr., Fairman, R., Robertson, J. G., Hail, M. E., Ho, H. T., Falk, P. J., and Villafranca, J. J. (1996) *Biochemistry 35*, 1423−1431.
34. Emanuele, J. J., Jin, H., Yanchunas, J., Jr., and Villafranca, J. J. (1997) *Biochemistry 36*, 7264−7271.
35. Yan, Y., Munshi, S., Leiting, B., Anderson, M. S., Chrzas, J., and Chen, Z. (2000) *J. Mol. Biol. 304*, 435−445.
36. Bertrand, J. A., Auger, G., Fanchon, E., Martin, L., Blanot, D., van Heijenoort, J., and Dideberg, O. (1997) *EMBO J. 16*, 3416−3425.
37. Gordon, E., Flouret, B., Chantalat, L., van Heijenoort, J., Mengin-Lecreulx, D., and Dideberg, O. (2001) *J. Biol. Chem. 276*, 10999−11006.
38. Bouhss, A., Dementin, S., Parquet, C., Mengin-Lecreulx, D., Bertrand, J. A., Le Beller, D., Dideberg, O., van Heijenoort, J., and Blanot, D. (1999) *Biochemistry 38*, 12240−12247.
39. Auger, G., van Heijenoort, J., Vederas, J. C., and Blanot, D. (1996) *FEBS Lett. 391*, 171−174.
40. Radzicka, A., and Wolfenden, R. (1995) *Methods Enzymol. 249*, 284−312.
41. Bartlett, P. A., and Marlowe, C. K. (1983) *Biochemistry 22*, 4618−4624.
42. Lipinski, C. A., Lombardo, F., Dominy, B. W., and Feeney, P. J. (1997) *Adv. Drug Delivery Rev. 23*, 3−25.

BI015567M